BEAM SYNTHESIS OF A C-BAND CIRCULARLY POLARIZED DUAL-REFLECTOR ANTENNA USING A RECONFIGURABLE SUBREFLECTOR

Marzieh. Mehri Dehnavi* (1), Jean-Jaques. Laurin (1)
(1) Poly-GRAMES Research Center, Department of Electrical Engineering École Polytechnique, Montréal, Québec, H3T1J4, Canada, http://www.grames.polymtl.ca

Abstract

In this work, the phase-only synthesis technique is used for beam shaping of a C-Band circularly polarized dual-reflector antenna. The synthesis relies on Particle Swarm Optimization (PSO) by using the element factors of a 100-elements reflectarray. The optimized results suffer from discontinuities in the reflectarray phase distribution, leading to degradation of the far-field patterns. This work proposes a solution to force a continuous phase distribution among the reflectarray surface during the optimization process. The beam scanning capability of the proposed algorithm is investigated by scanning the beam in the *uv* plane, by -0.05 and -0.1 along the main axes, and by 0.07 along a 45-degree diagonal. It is shown that the phase smoothing condition leads to significant improvement in the quality of the synthesized beams.

1. Introduction

Reconfigurable antennas have extensive usage in wireless communications such as radar, mobile, and satellite communication systems. They offer in-orbit reconfigurability for communications and broadcasting satellites [1]. Beam reconfigurability should meet precise specifications in terms of beamwidth, sidelobe level, and null positioning. In addition to steering, narrow beam shaping adapted to desired coverage is often required [2].

In [3], beam scanning of a dual-reflector antenna is proposed by adjusting the phase distribution of the sub-reflectarray using Near-Field Focusing (NFF) and Progressive Phase Shift (PPS) techniques. The proposed system has a limited phase synthesis capability due to the small size reflectarray of the dual reflector antenna. Therefore, there are some challenges in implementing the proper beam synthesis technique for the proposed dual-reflector antenna.

Different algorithms exist in the literature for beam synthesis purposes. Particle Swarm Optimization (PSO) and Genetic Algorithm (GA) known as evolutionary phase synthesis algorithms are widely used for antenna arrays. Compared to GA, PSO implementation is less complex and needs less computing time, while conducting global and local search simultaneously [4, 5]. This algorithm is found to be effective in electromagnetic problems and is widely used in the design of microwave and antenna components (e.g. [6]).
This work implements beam synthesis by introducing a phase-only synthesis PSO algorithm. The proposed algorithm gives the ability of beam scanning in uv-plane as well as beam shaping. Section 2 briefly describes the PSO algorithm as well as the procedure used to apply it in beam synthesis. In Section 3, the beam scanning capability of the proposed synthesis method is illustrated by comparing the PSO results obtained by MATLAB with those obtained with the simulation of the whole system in FEKO using a hybrid "Method of Moments (MoM) and Physical Optics (PO)" solution.

2. Beam Synthesis of Dual Reflector Antenna

2.1. PSO

PSO is an evolutionary algorithm inspired by the concept of the search of birds hunting for food [6]. The first step for implementing this algorithm is to define the population number. This is the number of "particles" moving in the search space to find the best solution to the problem. The best solution is the one giving the lowest cost value. The iterative algorithm stops the process when the best cost reaches the goal value, or when a maximum pre-defined iteration number is reached. The mean square error (MSE) between desired and synthesized patterns is used as a cost function to be minimized.

Each potential solution in the algorithm is called a 'particle'. In phase synthesis, the particle consists of a set of phase shifts to be applied to the all the reflectarray elements. In this paper, we consider a small reflectarray with 100 elements, so each particle is a vector of 100 unknown phase values. Each of these phases is comprised between $-\pi$ and π. The set of 100 phases in each particle is updated in each iteration. After the last iteration, the optimized phase distribution is used to calculate the far-field pattern.

2.2. Implementing Beam Synthesis Algorithm

This section describes the main process of the beam synthesis applied to the antenna system shown in Figure 1. This system includes a horn, a subreflector consisting of the reflectarray for which the phases have to be optimized, and a solid parabolic dish. The system operates in circular polarization (CP). See [7] for a description of the reconfigurable CP reflectarray elements. The size of the square subreflector is $3.67\lambda \times 3.67\lambda$ and the projected diameter of the dish in the yz -plane is 23λ (λ=42mm) at the design frequency of 7 GHz. The dish F/D ratio is 0.5 λ. The reflectarray has 10×10 square elements with a periodicity of 15.75mm in a square lattice. For such a small array, a large fraction of the elements is close to the array edges, so assuming identical far-field patterns for all the elements is inaccurate in the beam synthesis. The different element factors of each reflectarray elements are therefore important parameters to be considered.

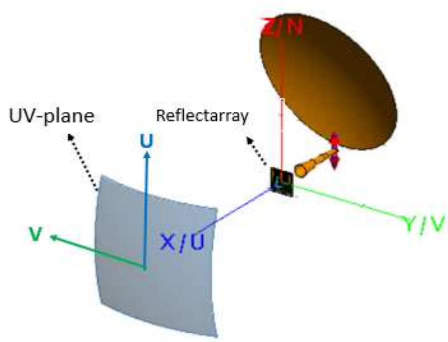

Figure 1. Dual reflector antenna including horn, sub-reflectarray and solid parabolic dish.

We define the element factor $f_n(u,v)$ as the contribution of the n[th] reflectarray element to the radiation pattern of the whole system. The far-field pattern is therefore a weighted sum of all the element factors as given by (1): .

$$F(u,v) = \sum_{n=1}^{N} |a_n| e^{j\varphi_n} f_n(u,v) \qquad (1)$$

where u and v are direction cosines in the far-field, as illustrated in the coordinate system shown on the left side of Figure 1. It should be noted that the "element pattern" is the far field of the whole system (horn, reflectarray and dish). These elements are obtained with 100 simulations of the system sitting at the same physical location. Therefore there is no need for the usual path length factors $\exp(j\beta \mathbf{r}_n' \bullet \hat{\mathbf{r}})$ in the sum. The element pattern is calculated for the reference state of the elements. In this state, the phases of the elements are adjusted using the standard path equalization reflectarray formula, is such a way that the reflected beam from the reflectarray is focused at the focal point of the dish. This state is related to the reference radiation pattern shown in Figure 2. In (1), a coefficient a_n is associated with each reflectarray element. The magnitude of a_n is set by the illumination intensity of the horn; the phase φ_n of the contribution of the n[th] element, can be controlled by element rotation. PSO finds the set of 100 phases $\{\varphi_n\}$, to generate a desired far-field pattern. The Mean Square Error (MSE) to be minimized is be based on the magnitude only of the normalized patterns:

$$MSE = \sum_{u,v} \left\| F_{d,norm}(u,v) \right| - \left| F_{norm}(u,v) \right\|^2 \qquad (2)$$

Where $F_{d,norm}$ is the normalized desired pattern and F_{norm} is the normalized optimized pattern. The obtained phase distribution $\{\varphi_n\}$ should be added to the reference phase state of the elements to realize the desired pattern. During the iterative process, MSE is calculated with 256 sample points in the uv -plane equally spaced in the range, $(u,v) = ([-0.3, 0.3], [-0.3, 0.3])$ as displayed in Figure 2.

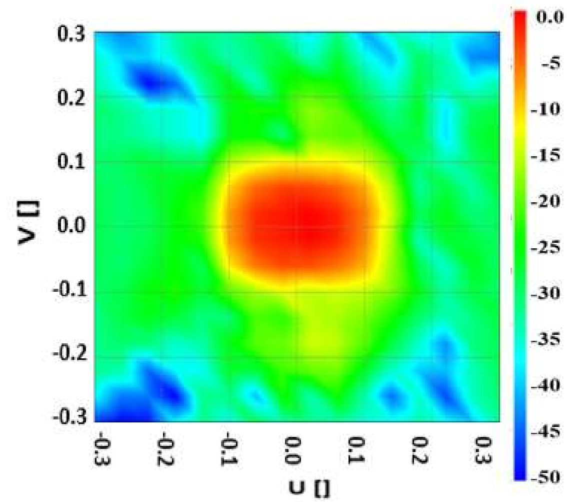

Figure 2. Reference Radiation Pattern

3. Discussion and Results

This section presents the results of the beam synthesis technique proposed in the previous section. For evaluating the performance of the algorithm, we first consider a simple problem where the reference pattern is defined as the desired pattern. The algorithm is started with a random phase distribution and is expected to converge to a proper phase distribution of 100 zero-phase ($\pm 2m\pi$) values. Zero phase distribution will not change the primary rotation angle of the elements and results in the reference pattern as the desired pattern. The PSO is implemented with a population number of 2000 and an iteration number of 5000. Figure 3 shows the convergence of MSE and Figure 4a shows the distribution of $\cos\varphi_n$ on the reflectarray elements, for the particle having the smallest MSE, after 5000 iterations. The figure shows a quasi-random phase distribution, which is far from the expected uniform phase. The normalized far-field pattern calculated by PSO is however close to the desired pattern. Using the phase calculated by PSO in the hybrid (MoM + PO) simulation of the antenna with FEKO, it is found that the resulting pattern, shown in Figure 4b, is quite different from the expected reference pattern of Figure 2.

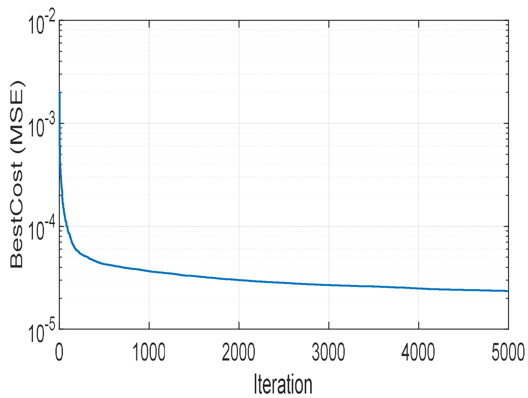

Figure 3. MSE of the optimized pattern with the reference pattern as desired pattern.

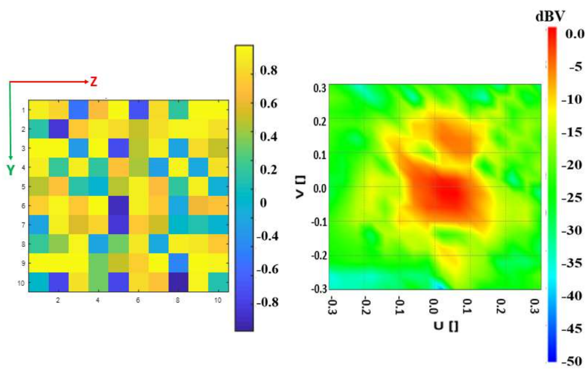

Figure 4. a) Distribution of $\cos\varphi_n$ on the reflectarray elements of the optimized pattern with the reference pattern as desired pattern. **b)** Radiation pattern obtained by hybrid simulation of the antenna in FEKO using the phase distribution in Figure 4a.

It was conjectured that the poor results obtained with the hybrid simulation come from the rapidly varying phase visible in Figure 4a. The phase response of reflectarray unit cells is generally calculated with the assumption of infinite arrays of identical cells, which is not the case when the phase varies rapidly and not linearly from cell to cell. To address the phase variation problem, a phase-smoothing term is added to the cost function to minimize the divergence of the phase gradient (i.e. Laplacian of $\exp(j\varphi_n)$). This is the last term in (3).

$$MSE = \sum_{u,v} \left\| \left| F_{d,normalized}(u,v) \right| - \left| F_{normalized}(u,v) \right| \right\|^2 + \alpha \sum_{i,j} \left| \nabla^2 \exp(j\varphi_{i,j}) \right| \quad (3)$$

Constant α is a regularization parameter to be adjusted, and $\sum_{i,j} \left| \nabla^2 \exp(j\varphi_{i,j}) \right|$ is Laplacian operator defined at element (i,j) of the reflectarray and calculated by using finite differences:

$$\nabla^2 \exp(j\varphi_{i,j}) \approx \exp(j\varphi_{i,j}) - \frac{1}{4}(\exp(j\varphi_{i-1,j}) + \exp(j\varphi_{i+1,j}) + \exp(j\varphi_{i,j-1}) + \exp(j\varphi_{i,j-1})) \quad (4)$$

In (4), each (x_i, y_j) point needs to have 4 neighbours in the grid, so the points on the corners and edges of the grid are excluded from the MSE calculation.

The validation case where the reference pattern is defined as the desired pattern was repeated with this new MSE function. The value of α is selected in the same range as the converged MSE value obtained in Figure 3. Figure 5a shows the phase distribution of the optimized pattern with the updated MSE using PSO. The value of α is 5×10^{-5}, the population number of 2000 and iteration number of 5000 for this example. The results indicate that the algorithm converged to the expected nearly-constant phase distribution. Figure 5a shows the cosine of the phase distribution, the yellow color illustrates phases of zero. Figure 5b shows the obtained radiation pattern by applying the phase distribution in Figure 5a.

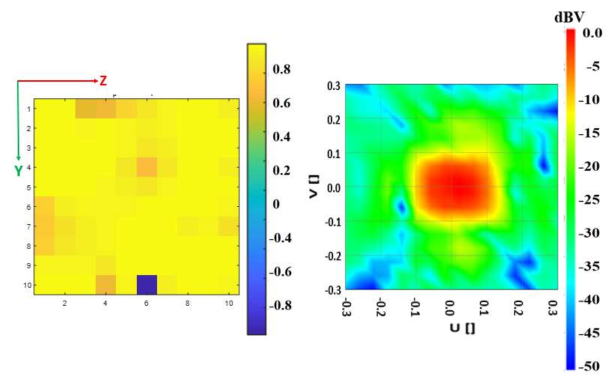

Figure 5. a) Distribution of $\cos\varphi_n$ on the reflectarray elements of the optimized pattern with the reference pattern as desired pattern, when adding a phase-smoothing term in the cost function. **b)** Radiation pattern obtained by simulation of the antenna in FEKO using the phase distribution $\{\varphi_n\}$ in Figure 5a.

The same population number and iteration number, as well as the same α value, were used to synthesize scanned beams. Beam steerings of +0.05, -0.1 along the v axis, and 0.07 at 45 degrees diagonally in uv-plane are provided. The radiation patterns obtained by PSO optimization in uv-plane for these scans are shown in Figure 6. Converged MSE values of 0.00169, 0.0014 and 0.00138 are obtained after 5000 iterations for Figures 6 a, b, c respectively.

The radiation patterns obtained from the PSO optimization are supported by comparing the results with the radiation pattern obtained by simulation in FEKO as provided in using the phases obtained from PSO, see Figure 7. Good agreement between the results in Figures 6 and 7 is observed.

The phase distributions of the optimized patterns on the reflectarray are shown in Figure 8. Progressive phase shift distribution is obtained in the v direction in Figure 8a and

8b. Moreover, a diagonal progressive phase shift can be observed for diagonal scanning as shown in Figure 8c.

4. Conclusion

This work demonstrates beam scanning by a dual-reflector antenna obtained with phase-only synthesis optimized with PSO. The algorithm leads to a quasi-random phase distribution on the reflectarray for the optimized pattern and does not result in the desired radiation pattern. The modified MSE function minimizes the Laplacian of the phase distribution. This modification provides more stable results and leads to scanned beams in the desired direction with regular contours.

5. Acknowledgements

The authors would like to acknowledge the support of MDA, Thales Canada, NSERC, CRIAQ and CARIC.

6. References

1. A. K. Bhattacharyya, "Projection Matrix Method for Shaped Beam Synthesis in Phased Arrays and Reflectors," in *IEEE Trans. Ant. and Propagat.*, vol. **55**, no. 3, pp. 675-683, March 2007.

2..A.K. Bhattacharyya, Phased array antennas: Floquet analysis synthesis. In BFNs and active array systems. Wiley-Interscience, 2006.

3. M.M. Dehnavi and J.-J. Laurin, "Beam scanning dual reflector antenna with a circularly polarized reconfigurable reflectarray as subreflector," in *70th Int. Astron, Cong. (IAC 2019)*, Washington, DC, USA, October 2019.

4. E. R. Schlosser, S. M. Tolfo and M. V. T. Heckler, "Particle Swarm Optimization for antenna arrays synthesis," *2015 SBMO/IEEE MTT-S Int.Microw. Optoel. Conf. (IMOC)*, pp. 1-6, Porto de Galinhas, Brazil, November, 2015.

5. L. A. Greda, A. Winterstein, D. L. Lemes and M. V. T. Heckler, "Beamsteering and Beamshaping Using a Linear Antenna Array Based on Particle Swarm Optimization," in *IEEE Access*, vol. **7**, pp. 141562-141573, September, 2019.

6. B. Kadri, et al. "Patterns antennas arrays synthesis based on adaptive particle swarm optimization and genetic algorithms," *Int. Jour. Comp. Sci. Issues,* 10, pp.21, March 2013.

7. M. M. Dehnavi and J. Laurin, "C-band circularly polarized reconfigurable reflectarray unit cells," *2017 XXXIInd URSI Gen. Ass, Sci, Symp. (URSI GASS)*, Montreal, Canada, pp. 1-4, August 2017.

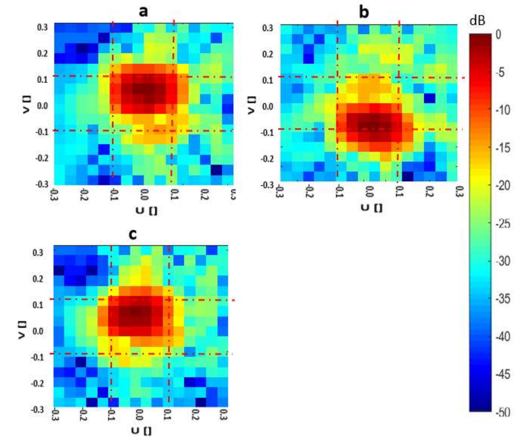

Figure 6. Normalized amplitude of the optimized patterns by PSO in MATLAB **a)** Δu=0, Δv=0.05 **b)** Δu=0, Δv=-0.1 **c)** Δu=-0.05, Δv=0.05.

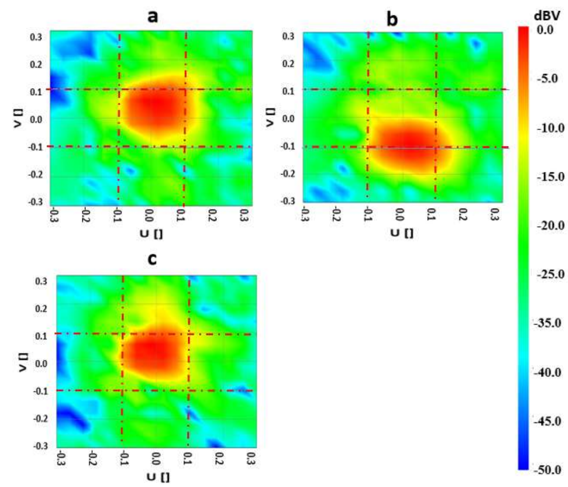

Figure 7. Normalized amplitude of radiation patterns obtained by hybrid simulation in FEKO **a)** Δu=0, Δv=0.05 **b)** Δu=0, Δv=-0.1 **c)** Δu=-0.05, Δv=0.05.

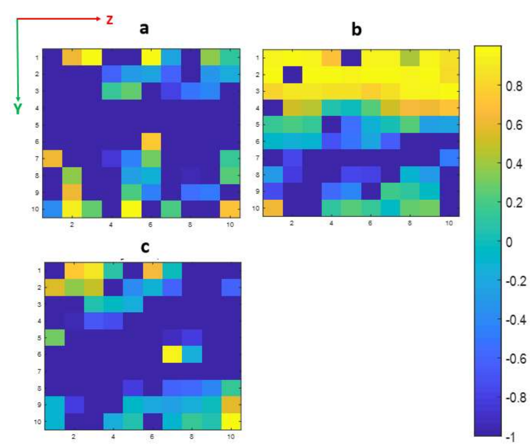

Figure 8. Distribution of $\cos\varphi_n$ on the reflectarray for optimized patterns: **a)** Δu=0, Δv=0.05 **b)** Δu=0, Δv=-0.1 **c)** Δu=-0.05, Δv=0.05.